International Journal of Advanced Engineering Research and Science (IJAERS)
Peer-Reviewed Journal
ISSN: 2349-6495(P) | 2456-1908(O)
Vol-9, Issue-6; Jun, 2022
Journal Home Page Available: https://ijaers.com/
Article DOI: https://dx.doi.org/10.22161/ijaers.96.31

A CHF Model for Pool Boiling on Rough Surface under Exponential Heat Supply

Avdhoot Walunj[1], Alangar Sathyabhama[2], Amol Mande[3], Ravindra Kolhe[4], Dattatray Palande[4]

[1]Department of Farm Machinery and Power Engineering, Mahatma Phule Krishi Vidyapeeth, Rahuri-413722, India
Email: aawalunj@gmail.com , avdhoot.walunj@nic.in
[2]Department of Mechanical Engineering, National Institute of Technology Karnataka, Surathkal-575025, India
Email : bhama72@gmail.com
[3]Department of Mechanical Engineering, Sanjivani College of Engineering, Kopargaon-423603, India
Email : mandeamolmech@sanjivani.org.in
[4]Department of Mechanical Engineering, Sanjivani College of Engineering, Kopargaon-423603, India
Email : kolheravindramech@sanjivani.org.in
[5]Department of Mechanical Engineering, Matoshri College of Engineering and Research Center, Nashik -422105, India
Email : dpalande@gmail.com

Received: 10 May 2022,

Received in revised form: 02 Jun 2022,

Accepted: 07 Jun 2022,

Available online: 15 Jun 2022

***Keywords*— surface roughness, transient heat transfer, heat transfer coefficient, hydrodynamic model**

***Abstract*—** *In present study, the experiments are carried on sample of different surface roughness to investigate the transient heat transfer phenomenon at the saturated condition of the distilled water. The surface roughness (R_a) ranges from 0.106 μm to 4.03 μm. The boiling crisis is observed during each transient heat supply. The high-speed camera of 1000 fps is used to observe the stages of boiling during different transient and to confirm the moment of critical heat flux (CHF). The empirical relation is presented for transient CHF and corresponding heat transfer coefficient (HTC). It is found that transient CHF is a function of both Ra and γ. The hydrodynamic model is developed for prediction of CHF at different rate of exponential heat supply for the wide range of Ra by incorporating γ.*

I. INTRODUCTION

The knowledge of boiling crisis in the nuclear reactors during exponential heat supply is important for the safety and efficient performance. The moment of critical heat flux (CHF) after which sharp reduction in heat transfer coefficient (HTC) is observed may lead to the rapid surge in the core temperature. Thus the formation of vapor blanket at CHF may lead to core meltdown accident. Hence understanding of the mechanism of transient CHF during exponential power escalation is of paramount importance. Researchers have contributed to explaining the CHF mechanisms by various approach viz. (i) Kelvin–Helmholtz instability between the upward flow vapor columns and downward flow liquid, (ii) dry-out of the liquid layer i.e. micro/macrolayer dry-out. Kutateladze [1] and Zuber [2] considered the Kelvin-Helmholtz instability as surface-fluid interaction fails due to relative motion between vapor column and surrounding liquid. Chang [3] considered the forces acting on the bubble during lift off from the horizontal surface and claimed that the critical velocity of the upward moving bubble is responsible for CHF. Haramura and Katto [4] stated near field evaporation phenomena through the macrolayer evaporation model and estimated CHF at the dry-out condition of macrolayer.

Lay and Dhir [5] and Pasamehmetoglu et al. [6] developed the theoretical model based on microlayer

evaporation. Zhao et al. [7, 8] developed steady-state and transient CHF model by considering various boiling aspects like time variant microlayer thickness, microlayer evaporation, macrolayer evaporation and transient conduction over the entire period of boiling. Hence, hydrodynamic models were coupled with surface-fluid properties like contact angle [9], surface roughness [10,11] and heater orientation [12]. The effects of boiling surface properties must be included in a robust and widely applicable CHF model. Kandlikar [11] proposed a force balance model which includes the contact angle of the bubble. Ahn et al. [13] included the term for capillary wicking in the Kandlikar's model to estimate the CHF. Quan et al. [14] proposed the force balance model, which includes roughness factor (r), to predict CHF for the micro structured surface. Kim et al. [15] developed the CHF model by considering capillary force, surface roughness (R_a) and static contact angle. The capillary force through the unidirectional scratches was predicted by assuming number of capillary tubes underneath the growing bubble. It is noticed from the literature that theoretical model can be developed from force balance approach to predict the CHF. Far-field and near-field models are developed by considering surface roughness (R_a), roughness parameter r, static contact angle, surface wetting property, surface orientation and heater size. In the present study, influence of surface roughness R_a and period of exponential heat supply on transient CHF is studied. A pioneering study is carried to include new term, so-called time constant γ in the CHF model.

II. EXPERIMENTATION

2.1 Experimental Setup

A boiling chamber with the test section and condenser assembly include in the experimental setup. The schematic of experimental setup and visualization unit is shown in Fig. 1. The detachable top and bottom flange are provided to the boiling chamber. The condenser coil is attached to the top flange whereas bottom flange can accommodate the test section assembly. The bulk fluid temperature (T_l) and chamber pressure are measured by the thermocouple and pressure transducer, respectively. The transparent toughened borosilicate glass watch windows of 115 mm diameter and 15 mm thickness are provided to the wall of boiling chamber to conduct the visualization study by high speed camera. The saturation condition of the distilled water is maintained by the two high density cartridge heaters each of 1000W capacity. The setup is synchronized with high speed camera, NI-9213 temperature module and NI-9264.

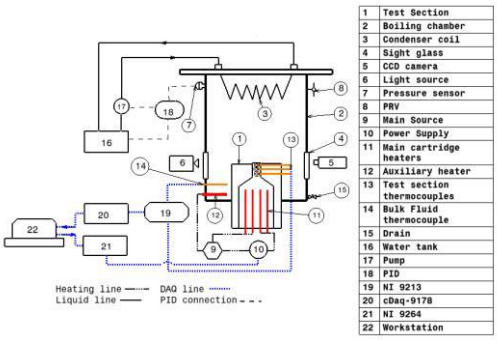

Fig. 1: Experimental Setup

2.2 Test Section

Thick copper sample of 20 mm length and the diameter of 20 mm is prepared as shown in Fig. 2. The 840 W high density cartridge heater is used to supply the heat. The thermal paste is applied on both the contact surfaces and thereafter, sample is screwed with the heating block which ensures the perfect surface contact between them. The glass wool insulation is provided over the sample and heating block. An O-ring and high-temperature non-corrosive RTV silicone gasket ensures the leak proof assembly. Three K-type sheathed thermocouples of 1 mm diameter are implanted from the top of the sample surface at 2 mm, 6 mm, and 10 mm.

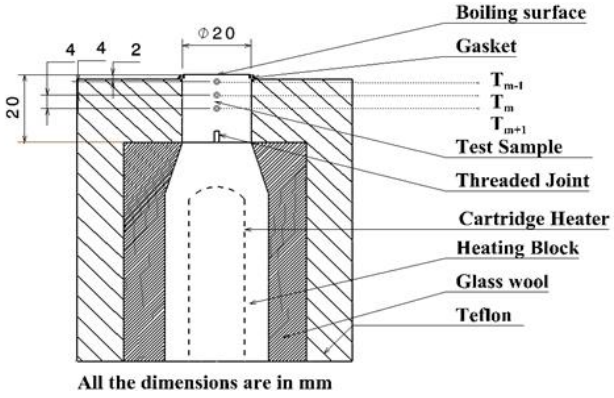

Fig. 2 : Test Section

2.3 Experimental Procedure

The assembly of test section is considered as the axisymmetric system. The uniform heat flux from the boiling surface is assumed due to uniform surface characteristics. The heat flux dissipated to the boiling fluid and the surface temperature can be measured using thermocouple.

The time variant heat flux from the boiling surface due to exponentially varying heat supply is calculated by Equation 1.

$$q_{ts}^{"} = -k_{Cu}\frac{T_{m-1}^{t} - T_{m+1}^{t}}{2\Delta x} \quad (1)$$

where Δx is the gap between two adjacent implanted thermocouples.

The temperature of the boiling surface is calculated by using Equation 2.

$$T_{w}^{t} = T_{m-1}^{t} - q_{ts}^{"}\left(\frac{x_{m-1}}{k_{Cu}}\right) \quad (2)$$

where, x_{m-1} is the gap between boiling surface and the thermocouple (T_{m-1}), as given in Fig. 2.

Heat transfer coefficient (HTC) between the boiling surface and water is estimated by Equation 3.

$$h_{ts} = \frac{q_{ts}^{"}}{(T_{w}^{t} - T_{l})} \quad (3)$$

The values of uncertainty in the measured and estimated parameters are given in Table 1.

The values of uncertainty in the measured and estimated parameters are given in Table 1.

Table 1 : Uncertainties of measured and calculated parameters

Parameter	Uncertainty
T	±0.1°C
x	±0.0001 m
P	0.2 %
heat flux	11.91 %
HTC	16.20 %

III. RESULTS AND DISCUSSION

The roughness parameters of the test sample, which were measured before and after boiling tests, are tabulated in Table 2. The R_a value of the test sample is considered as the roughness parameter in this study.

Table 2 : Roughness parameters in μm

R_a	R_z	R_q	S_m
0.106	1.20	0.14	13.2
0.83	7.05	1.07	26.8
1.87	13.30	2.40	35.7
3.17	22.91	4.12	42.2
3.59	27.55	4.09	44.8
4.03	26.50	4.95	45.2

The experiments are conducted on different samples with exponentially varying heat supply and respective boiling curves are obtained. Effect of roughness on transient boiling heat transfer is noticed in the boiling curves obtained for γ=3, as shown in Fig. 3. It is clearly found that boiling curves moves onto the left with increase in values of Ra, indicating that the heat transfer enhancement is due to the rough surface. The heat transfer enhancement due to rough surface can be justified by the mechanism of liquid replenishment and surface wettability. Unidirectional scratches made on the surface act as a passage for liquid supply to the nucleation sites. The wetting property of the surface also improved due to capillary wicking along the scratches. The irregularities increase with Ra which has more potential to be nucleation sites. Thus increased number of bubble and the improved liquid supply mechanism to the nucleation sites resulted in heat transfer augmentation. Also, the nucleation boiling temperature is found to be decreased with increase in values of Ra. The activation of pre-existing vapor in the cavities of rough surface results in formation of bubble at lower wall superheat.

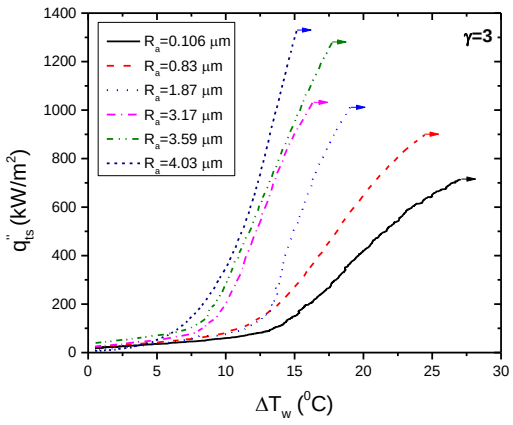

Fig. 3: Boiling curves of the test samples at γ=3

It is observed during visualization study that exponentially increasing heat supply creates the instability in the bubble formation. The waiting period between two successive bubbles drops drastically with increase in rate of heating. Thus, sudden increase in the bubble frequency results in the vertical bubble coalescence. Formation of vapor column is observed during visualization at this stage, as shown in Fig. 4. This mechanism of bubble formation decreases the heat transfer rate from the surface. Hydrodynamic instability affects the liquid replenishment adversely which turn to horizontal bubble coalescence. Thus, the blanket of vapor occupies the entire boiling surface. The transition mechanism of nucleated bubble from the fully developed nucleate boiling (FDNB) regime to the film boiling results in drop of HTC. This transition point of boiling curve which corresponds to the maximum

HTC is identified as CHF. The transient CHF and corresponding HTC is presented in Fig. 5 and Fig. 6, respectively, at different Ra and γ. The values of $q''_{CHF,ts}$ are plotted against Ra and γ separately and exponents are obtained. The final relation for $q''_{CHF,ts}$ as a function of Ra and γ is derived as given in Equation 4 by least square regression. It is believed that $h_{max,ts}$ is a function of $q''_{CHF,ts}$, Ra and γ. The relation developed for $h_{max,ts}$ is given in Equation 5.

$$q''_{CHF,ts} = 1031.9\ (\gamma)^{-0.08}(R_a)^{0.14} \quad (4)$$

$$h_{max,ts} = 0.04\ (\gamma)^{-0.07}(R_a)^{0.17}\left(q''_{CHF,ts}\right)^{1.04} \quad (5)$$

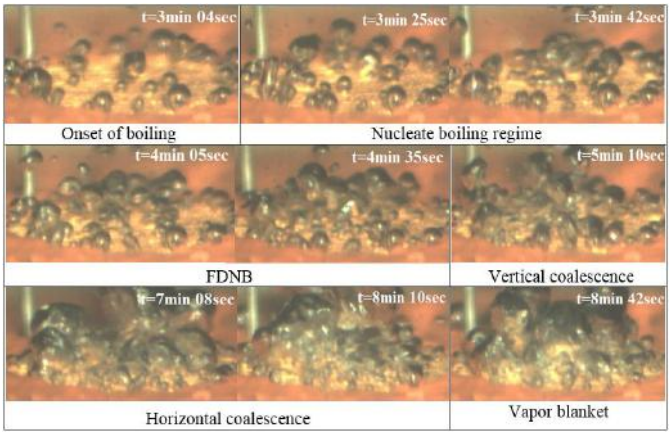

Fig. 4 : Boiling stages for Ra =3.19 μm and γ=1

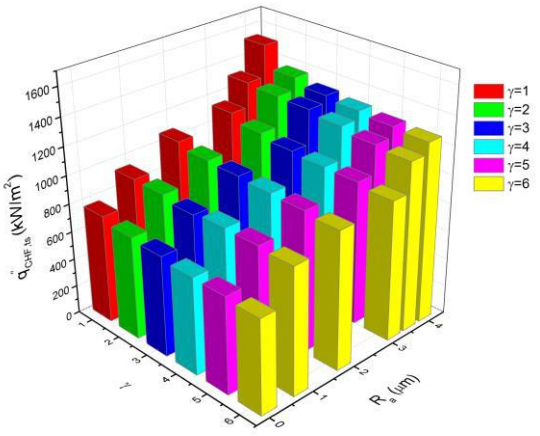

Fig. 5 Variation in $q''_{CHF,ts}$ with Ra and γ

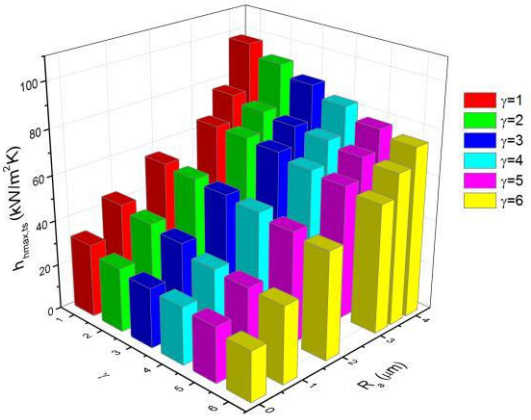

Fig. 6 Variation in $h_{max,ts}$ with Ra and γ

IV. HYDRODYNAMIC MODEL

The bubble formed on the upward facing rough surface experiences the forces as shown in Fig. 7. Force due to change in the momentum (FM) acts on the bubble circumference which pulls the bubble along the surface. Simultaneously, bubble position retains due to forces like surface tension force, gravity and capillary force acting on it. It is observed during present study that horizontal coalescence is responsible to turn FDNB to film boiling regime. This transition in phase of boiling occurs when FM surpasses the sum of drag forces. The moment of CHF is identified by the force balance as given in Equation (6).

$$F_M = F_{s,t} + F_{s,b} + F_g + F_c \quad (6)$$

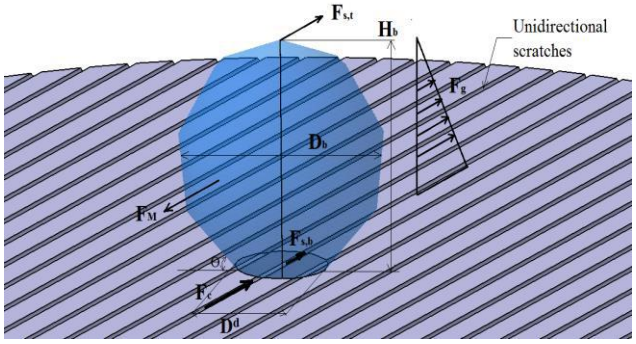

Fig. 7 : Forces acting on the bubble along the surface

A developing bubble, due to its change in momentum, experiences a force on its meniscus. The change in momentum (F_M) causes due to continual liquid is estimated as given in Equation 7.

$$F_M = \frac{1}{\rho_v}\left(\frac{q''_l}{h_{fg}}\right)^2 H_b \quad (7)$$

The surface tension forces acting at top ($F_{s,t}$) and bottom ($F_{s,b}$) of the bubble, are given in equation 8, respectively.

$$F_{s,t} = \sigma \, ; F_{s,b} = \sigma \cos\theta \quad (8)$$

The gravity force (F_g) which acts on the boiling surface is given in Equation 9.

$$F_g = \frac{1}{2} g(\rho_l - \rho_v) H_b^2 \quad (9)$$

The capillary force (F_c) which acting on the bubble, as given in Equation 10, for capillary pressure acting inside the small tube of radius R_c. It is assumed that unidirectional scratch is a capillary tube and many such capillary tubes may lies below the growing bubble.

$$F_c = 2\pi C \left(\frac{R_a}{S_m}\right) \sigma \cos\theta \quad (10)$$

Combining all the above forces, q''_l is expressed by Equation 11.

$$q''_l = h_{fg}\rho_v{}^{0.5} \left[\sigma g(\rho_l - \rho_v)\right]^{0.25} \left[\frac{2}{\pi} + \frac{\pi}{4}(1+\cos\theta) + \frac{4C\cos\theta}{1+\cos\theta}\left(\frac{R_a}{S_m}\right)\right]^{0.5} \quad (11)$$

Steady-state CHF can be obtained by the Equation 12 as suggested by Kandlikar [11]

$$q''_{CHF,ss} = \left(\frac{1+\cos\theta}{16}\right) q''_l \quad (12)$$

The relation developed between steady-state CHF and R_a is given in Equation 13.

$$q''_{CHF,ss} = 1280.8 \times R_a{}^{0.14} \quad (13)$$

The relation between $q''_{CHF,ts}$ and q''_l is obtained and the final form of CHF model for exponential heat supply ranging from γ=1 to γ=6 for wide range of surface roughness R_a is given in Equation 14.

$$q''_{CHF,ts} = \left(\frac{0.81}{\gamma^{0.08}}\right)\left(\frac{1+\cos\theta}{16}\right)\left\{h_{fg}\rho_v{}^{0.5}\left[\sigma g(\rho_l - \rho_v)\right]^{0.25}\right\}\left[\frac{2}{\pi} + \frac{\pi}{4}(1+\cos\theta) + \frac{4C\cos\theta}{1+\cos\theta}\left(\frac{R_a}{S_m}\right)\right]^{0.5} \quad (14)$$

Fig. 8 illustrate the comparison between experimental data and the predicted transient CHF values obtained from Equation 14 and mean absolute error (MAE) is estimated which found to be 4.05%. The term of γ present in the denominator suggest that difference between steady and transient CHF will increase with increase in the γ.

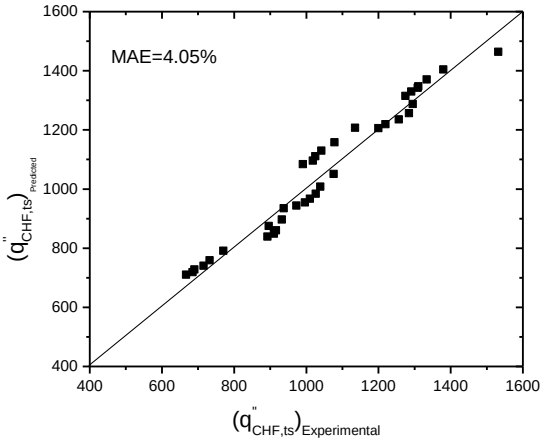

Fig.8 Comparison of $q''_{CHF,ts}$ obtained by present model with experimental $q''_{CHF,ts}$

V. CONCLUSION

An extensive study of pool boiling on copper surface with wide range of surface roughness Ra under different rate of exponential heat supply was carried to understand the physical mechanism and parametric dependence of transient CHF. It is observed that transient CHF increases with increase in Ra whereas it decreases with increase in γ. A transient CHF model is developed by including time constant γ to account for the influence of exponential heat supply on the CHF. The present model predicts the experimental values of transient CHF with MAE=4.05%.

REFERENCES

[1] S.S. Kutateladze, On the transition to film boiling under natural convection, Kotloturbostroenie 3 (1948) 152–158.

[2] N. Zuber, Hydrodynamic aspects of boiling heat transfer, AECU-4439, 1959.

[3] Chang, Y. P. (1961) An Analysis of the Critical Conditions and Burnout in Boiling Heat Transfer, USAEC Rep. TID-14004, Washington, DC.

[4] Y. Haramura, Y. Katto, A new hydrodynamic model of critical heat flux, applicable widely to both pool and forced convection boiling on submerged bodies in saturated liquids, Int. J. Heat Mass Transfer 26 (1983) 389–399.

[5] J.H. Lay, V. K. Dhir. (1995) Shape of a vapor stem during nucleate boiling of saturated liquids, Trans. ASME J. Heat Transfer 117, 394–401.

[6] K.O. Pasamehmetoglu, P.R. Chappidi, C. Unal, R.A. Nelson. (1993). Saturated pool nucleate boiling mechanisms at high heat fluxes, Int. J. Heat Mass Transfer 36, 3859–3868.

[7] Y.H. Zhao, T. Masuoka, T. Tsuruta. (2002). Unified theoretical prediction of fully developed nucleate boiling and critical heat flux based on a dynamic micro layer model, Int. J. Heat Mass Transfer 45, 3189–3197.

[8] Y.H. Zhao, T. Masuoka, T. Tsuruta. (2002). Theoretical studies on transient pool boiling based on microlayer model, Int. J. Heat Mass Transfer 45, 4325–4331.
[9] Yu.A. Kirishenko, P.S. Cherniakov. (1973). Determination of the first critical thermal heat flux on flat heaters, J. Eng. Phys. 20, 699–702.
[10] J.J. Wei, H. Honda. (2003). Effects of fin geometry on boiling heat transfer from silicon chips with micro-pin-fins immersed in FC-72, Int. J. Heat Mass Transfer 46, 4059–4070.
[11] S. G. Kandlikar. (2001). A Theoretical model to predict pool boiling CHF incorporating effects of contact angle and orientation, J. Heat Transfer 123, 1071–1079.
[12] A. H. Howard, I. Mudawar. (1999). Orientation effects on pool boiling critical heat flux (CHF) and modeling of CHF for near-vertical surfaces, Int. J. Heat Mass Transfer 42, 1665–1688.
[13] H. S. Ahn, H. J. Jo, S.H. Kang, M.H. Kim. (2011). Effect of liquid spreading due to nano/ microstructures on the critical heat flux during pool boiling, Appl. Phys. Lett. 98, 071908.
[14] X. Quan, L. Dong, P. Cheng. (2014). A CHF model for saturated pool boiling on a heated surface with micro/nano-scale structures, Int. J. Heat Mass Transfer 76, 452–458.
[15] J. Kim, S. Jun, R. Laksnarain, S. M. You. (2016). Effect of surface roughness on pool boiling heat transfer at a heated surface having moderate wettability, Int. Journal of Heat and Mass Transfer 101, 992–1002.